Ionized Physical Vapor Deposition (IPVD): Technology and Applications

Jón Tómas Guðmundsson

Science Institute, University of Iceland, Iceland
Department of Electrical and Computer Engineering, University of Iceland, Iceland
tumi@hi.is

10th International Symposium on Sputtering and Plasma Processes (ISSP)
Kanazawa, Japan, July 8., 2009

Introduction

- The demand for new materials and layer structures has lead to development of more advanced sputtering systems
  - in particular to increase the ionization of the sputtered vapor
  - traditionally by adding a secondary discharge between the target and the substrate
- A recent addition is the
  - high power pulsed magnetron sputtering discharge (HPPMS)
  - high power impulse magnetron sputtering discharge (HiPIMS)
- It gives high electron density and highly ionized flux of the sputtered material

Outline

- Magnetron Sputtering Discharge
- Ionized Physical Vapor Deposition (IPVD)
- High power impulse magnetron sputtering discharge (HiPIMS)
  - Power supply
  - Electron density
  - Plasma dynamics
  - Electron energy
  - Ionization fraction
  - Ion energy
  - Deposition rate
  - Applications
- Summary

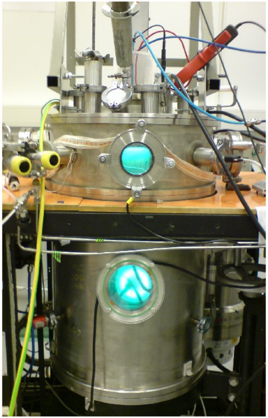

Planar Magnetron Sputtering Discharge

Planar Magnetron Sputtering Discharge

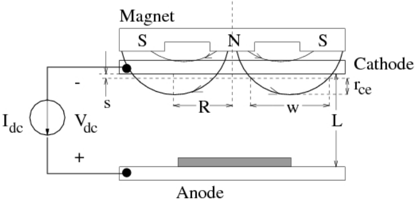

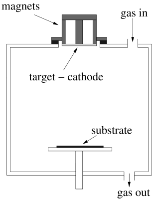

- For a typical dc planar magnetron discharge
  - pressure of 1 – 10 mTorr
  - a magnetic field strength of 0.01 – 0.05 T
  - cathode potentials 300 – 700 V
  - average power 200 – 600 W
  - electron density in the substrate vicinity is $10^{15} - 10^{17}$ m^{-3}
  - low fraction of the sputtered material is ionized $\sim$ 1 %
  - the majority of ions are the ions of the inert gas
  - the sputtered vapor is mainly neutral

Planar Magnetron Sputtering Discharge

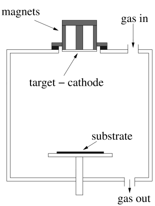

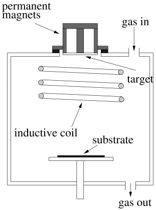

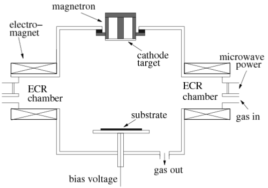

- In magnetron sputtering discharges increased ionized flux fraction is achieved by
    - a secondary discharge between the target and the substrate (rf coil or microwaves)
    - reshaping the geometry of the cathode to get more focused plasma (hollow cathode)
    - increasing the power to the cathode (high power pulse)
- Common to all highly ionized magnetron sputtering techniques is a very high density plasma

Ionized Physical Vapor Deposition (IPVD)

Ionized Physical Vapor Deposition (IPVD)

- When the flux of ions is higher than the flux of neutrals or $\Gamma_\mathrm{i} > \Gamma_\mathrm{m}$ the process is referred to as ionized physical vapor deposition (IPVD)
- The metal ions can be accelerated to the substrate by means of a low voltage dc bias
  - The metal ions arrive at the substrate at normal incidence and at specific energy
  - The energy of the ions can be tailored to obtain impinging particles with energies comparable to typical surface and molecular binding energies

Ionized Physical Vapor Deposition (IPVD)

- Ionizing the sputtered vapor has several advantages:
  - improvement of the film quality, increased film density (Kusano, 2006; Lim et al., 2000; DeKoven et al., 2003)
  - improved adhesion (Ehiasarian et al., 2007)
  - improved surface roughness (Sarakinos et al., 2007)
  - deposition on substrates with complex shapes and high aspect ratio (Alami et al., 2005)
  - phase tailoring (Alami et al., 2007)
  - guiding of the deposition material to the desired areas of the substrate (Bohlmark et al., 2006)
  - hysteresis free reactive sputtering has been demonstrated in a HiPIMS discharge (Wallin and Helmersson, 2008)

Ionized Physical Vapor Deposition (IPVD)

- The system design is determined by the average distance a neutral particle travels before being ionized
- The ionization mean free path is

$$\lambda_{\mathrm{iz}} = \frac{v_{\mathrm{s}}}{k_{\mathrm{iz}} n_{\mathrm{e}}}$$

where

  - v_{s} is the velocity of the sputtered neutral metal
  - k_{iz} is the ionization rate coefficient
  - n_{e} is the electron density

Ionized Physical Vapor Deposition (IPVD)

- This distance has to be short
  - v_s has to be low - thermalize the sputtered flux - increase discharge pressure
  - n_e has to be high
- Typical parameters for argon gas and copper target

Gas	v_s [m/s]	T_e [V]	n_e [m^{-3}]	λ_{iz} [cm]	Discharge
Ar	1000[a]	3	10^{17}	162	
Ar	300	3	10^{17}	49	dcMS
Ar	300	3	10^{18}	4.9	ICP-MS/ECR-MS
Ar	300	3	10^{19}	0.5	HiPIMS
Cu	300	1.5	10^{19}	7.5	SSS-HiPIMS

[a] (Britun et al., 2008)

Ionized Physical Vapor Deposition (IPVD)

- Another important parameter is the fraction of ionized metal flux

$$\frac{\Gamma_i}{\Gamma_i + \Gamma_n}$$

- The ion flux to the substrate is

$$\Gamma_i \approx 0.61 n_{m+} u_B \sim \sqrt{T_e}$$

- The flux of thermalized neutrals is

$$\Gamma_n = \frac{1}{4} n_m v_{Th} \sim \sqrt{T_g}$$

- Since $T_e \gg T_g$ the fraction of ionized metal flux is larger than the fraction of ionized metal in the plasma
- It is not necessary to completely ionize the sputtered metal to create a highly ionized flux to the substrate

High Power Impulse Magnetron Sputtering (HiPIMS)

High Power Impulse Magnetron Sputtering (HiPIMS)

- In a conventional dc magnetron discharge the power density is limited by the thermal load on the target
- In a HiPIMS discharge a high power pulse is supplied for a short period
  - low frequency
  - low duty cycle
  - low average power
- The high power pulsed magnetron sputtering discharge uses the same sputtering apparatus except the power supply

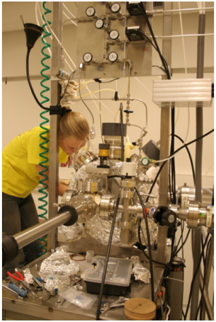

HiPIMS - Power supply

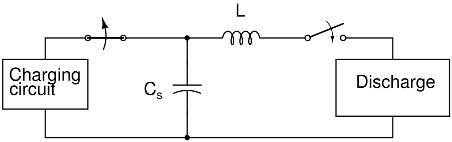

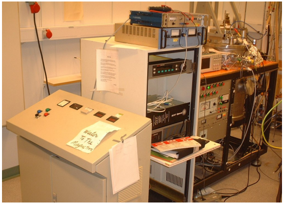

- The high power pulsed discharge operates with a
  - Cathode voltage in the range of 500 – 2000 V
  - Current densities of 3 – 4 A/cm^2
  - Power densities in the range of 1 – 3 kW/cm^2
  - Average power 200 – 600 W
  - Frequency in the range of 50 – 1000 Hz
  - Duty cycle in the range of 0.5 – 5 %

HiPIMS - Power supply

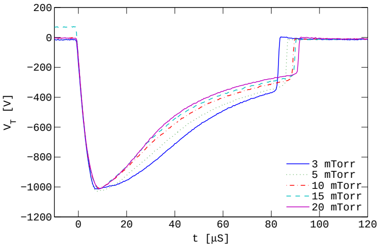

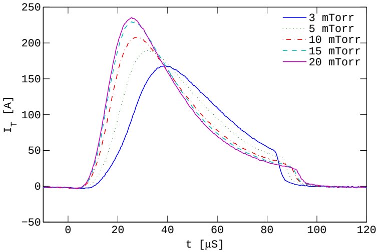

(From Sigurjonsson et al. (2009))

- The exact pulse shape is determined by the load
  - the discharge formed
  - it depends on the gas type and gas pressure

High Power Impulse Magnetron Sputtering (HiPIMS) - Electrons

Plasma parameters - Langmuir probe

- A Langmuir probe was used to study the temporal and spatial variation of the plasma parameters
  - electron density
  - electron energy
- For each voltage step the current drawn by the probe was measured as a function of time

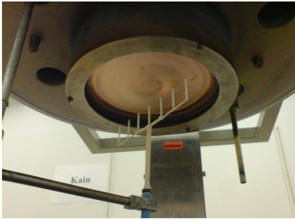

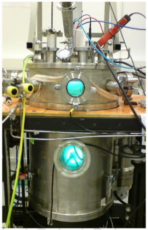

HiPIMS - Electron density

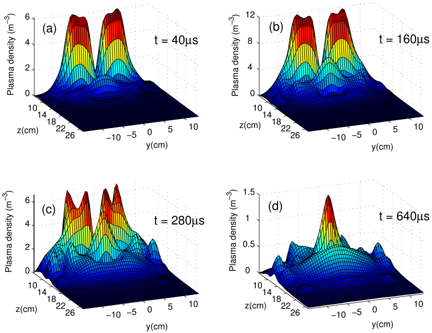

(After Bohlmark et al. (2005) and Guðmundsson et al. (2006))

- Temporal and spatial variation of the electron density
- Ar discharge at 20 mTorr, Ti target, pulse length 100 μs
- The electron density in the substrate vicinity is of the order of $10^{18} - 10^{19}$ m^{-3}

HiPIMS - Electron density

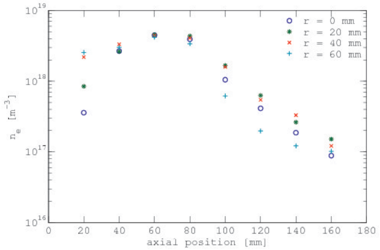

65 μs

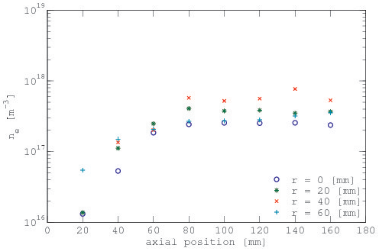

230 μs

(From Sigurjonsson et al. (2009))

- The spatial variation of the electron density at 65 μs and 230 μs from the initiation for gas pressure of 10 mTorr.
- The pulse is 90 μs long and the average power 270 W and the target made of copper
- The electron density is uniform along the radius of the discharge

HiPIMS - Electron density

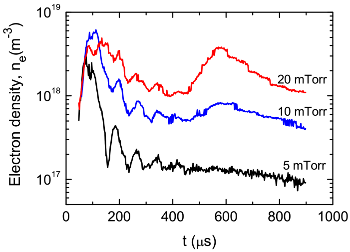

(After Gudmundsson et al. (2002))

- The electron density versus time from the initiation of the pulse 9 cm below the target
- The pulse is 100 μs long and the average power 300 W and the target made of tantalum
- A strong initial peak appears
- A second peak appears later in time at higher pressure

HiPIMS - Plasma dynamics

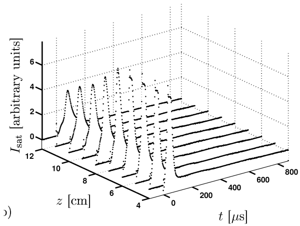

5 mTorr

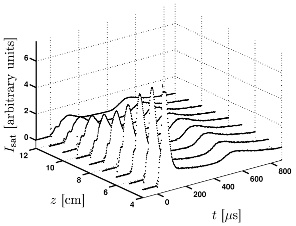

20 mTorr

(From Gylfason et al. (2005))

- The electron saturation current as a function of location and time from pulse initiation
- The argon pressure was 5 mTorr and 20 mTorr, the target was made of titanium, and the pulse energy 6 J

HiPIMS - Plasma dynamics

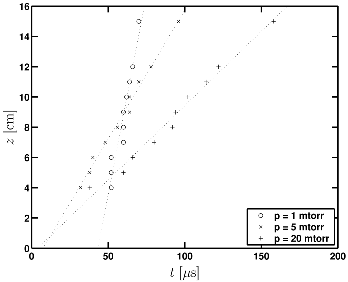

(From Gylfason et al. (2005))

- Each peak travels with a fixed velocity through the chamber
- The peaks travel with a velocity of 5.3×10^3 m/s at 1 mTorr, 1.7×10^3 m/s at 5 mTorr, and 9.8×10^2 m/s at 20 mTorr

HiPIMS - Plasma dynamics

- The plasma density versus time while varying the
  - sputtering gas
  - chamber dimension
  - distance to target
  - applied power
- The first peak appears immediately after the plasma ignition
- The peaks increase with increased applied power

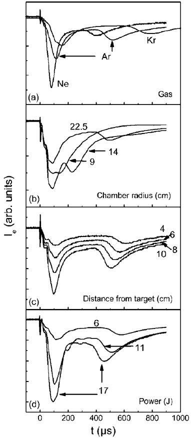

(From Alami et al. (2005))

HiPIMS - Plasma dynamics

- The second peak appears only for pressures above 5 mTorr
- The lighter the gas atom the earlier the peaks appear
- Decreased chamber radius results in earlier appearance of the second peak
    - we propose that the charged particles travel as sound waves
    - the second peak is a reflection from the walls

(From Alami et al. (2005))

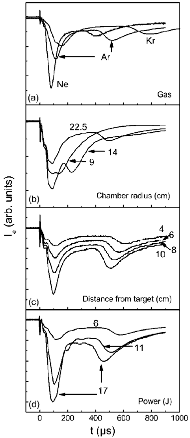

HiPIMS - Electron density

- The electron density depends on the target material
  - Cr target gives higher density than Ti
  - higher $[Cr^+]/[Ar^+]$ than $[Ti^+]/[Ar^+]$ ratio
- The ionization of metal atoms plays an important role in the creation of electrons

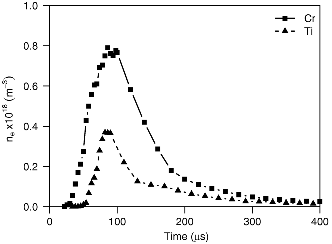

(From Vetushka and Ehiasarian (2008))

HiPIMS - Electron energy

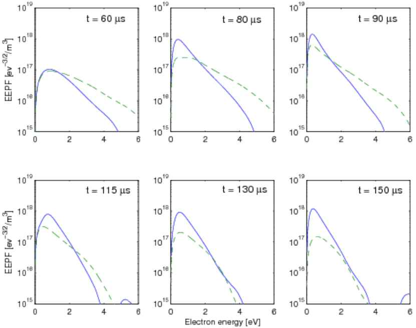

From Gudmundsson et al. (2009)

- The electron energy probability function (EEPF) under the race-track 100 mm below the target for an argon discharge at 3 (dashed) and 20 (solid) mTorr with a copper target

HiPIMS - Electron energy

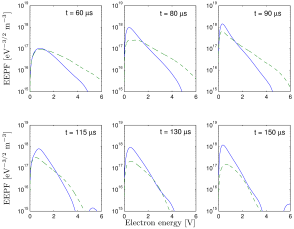

From Gudmundsson et al. (2009)

- The measured EEPF is Maxwellian-like during the pulse
  - high electron density leads to a Maxwellian-like low energy part of the EEPF
  - the depletion in the high energy part is due to the escape of high energy electrons to the chamber walls and inelastic collisions of high energy electrons
- The EEPF is more broad at low pressure and early in the pulse

HiPIMS - Electron energy

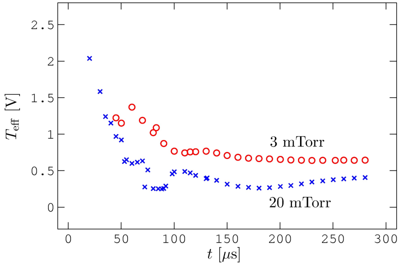

From Gudmundsson et al. (2009)

- Temporal variation of the effective electron temperature 100 mm below the target under the race-track ($r = 40$ mm)
- The electron energy decreases with increased discharge pressure

HiPIMS - Electron density - summary

- The peak electron density is of the order of $10^{18} - 10^{19}$ m^{-3}

  Gudmundsson et al. (2001, 2002); Bohlmark et al. (2005)
- A monotonic rise in plasma density
  - with discharge gas pressure

    (Gudmundsson et al., 2002)
  - applied power (Alami et al., 2005)
- A linear increase in electron density with increased discharge current

  (Ehiasarian et al., 2008)

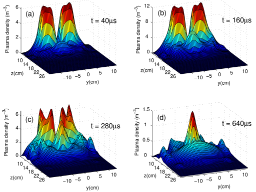

(After Bohlmark et al. (2005))

HiPIMS - Electrons - summary

- The electron density depends on the target material
  - Cr target gives higher density than Ti

    (Vetushka and Ehiasarian, 2008)
- The peak electron density travels away from the target with fixed velocity

  (Gylfason et al., 2005)
- The electron energy distribution function (EEDF) during the pulse is Maxwellian-like (Gudmundsson et al., 2009)

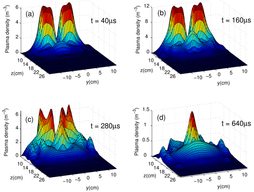

(After Bohlmark et al. (2005))

High Power Impulse Magnetron Sputtering (HiPIMS) - Ions

HiPIMS - Ionization fraction

- Conventional dc magnetron discharge - Pre-ionization - violet argon discharge
- HiPIMS discharge averaged over several pulses - green discharge characteristic of Cu vapour
- The Cu^{+} lines are only observed in HiPIMS mode

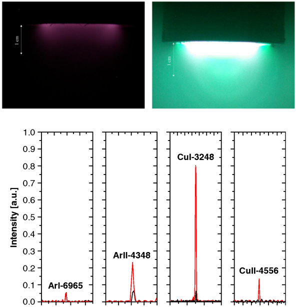

(From Vašina et al. (2007))

HiPIMS - Ionization fraction

- There have been conflicting reports on the fraction of ionized metal flux
  - 70 % for Cu (Kouznetsov et al., 1999)
  - 56 % for Cu (Vlček et al., 2007a)
  - 99 % for Ti (Kudláček et al., 2008)
  - 40 % for $Ti_{0.5}Al_{0.5}$ (Macák et al., 2000)
  - 9.5 % for Al (DeKoven et al., 2003)
  - 4.5 % for C (DeKoven et al., 2003)
- The degree of ionization
  - 90 % for Ti (Bohlmark et al., 2005)
- The fraction of ionized metal flux depends on applied power, pulse frequency and pulse length, and distance from the target

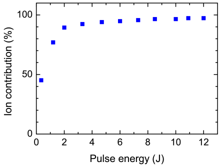

(From Bohlmark et al. (2005))

HiPIMS - Ionization fraction

- The ion flux versus time measured by a mass spectrometer (20 μs windows)
- The gas pressure was 3 mTorr, pulse energy 8 J and the target made of Ti
- Highly metallic ion flux during the active phase of the discharge

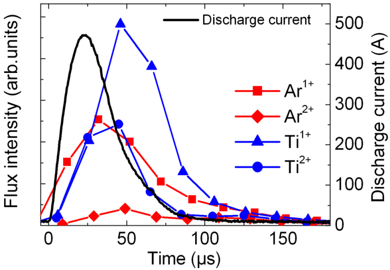

(From Bohlmark et al. (2006))

HiPIMS - Ionization fraction

- The discharge develops from an argon dominated discharge to a metal dominated discharge during the active phase of the discharge.
- This has been observed both by optical emission spectroscopy and mass spectroscopy
- Cu-ions have been measured to be up to 92 % of the total ion flux at the substrate (Vlček et al., 2007)
- Ti-ions are up to 29 % of the total ion flux at the same conditions

(Kudláček et al., 2008)

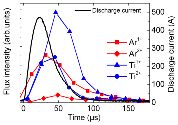

From Bohlmark et al. (2006)

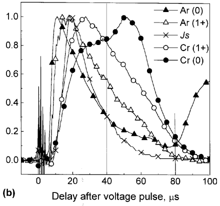

From Ehiasarian et al. (2002)

HiPIMS - Ionization fraction

- During the initial stages of the pulse Ar^{+} ions dominate the discharge
- Later in the pulse metal ions build up and become the abundant ion species
- Multiply charged ions have been observed
- Significant fraction of the ion flux is Ti^{2+} (Bohlmark et al., 2006)
- Ti^{4+} ions have been observed (Andersson et al., 2008)

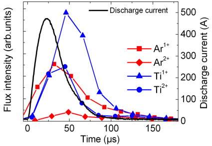

From Bohlmark et al. (2006)

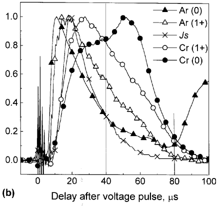

From Ehiasarian et al. (2002)

HiPIMS - Ion energy

- The time averaged ion energy distribution for Ar^+ and Ti^+ ions
- The gas pressure was 3 mTorr, pulse energy 3 J and 10 J and the target made of Ti
- The ion energy distribution is broad to over 100 eV
- About 50 % of the Ti^+ ions have energy > 20 eV

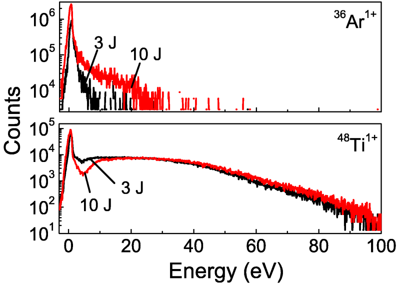

(From Bohlmark et al. (2006))

HiPIMS - Ion energy

- Significant fraction of the Ti^{+} ions are transported radially outwards
- Direction dependent high energy-tail

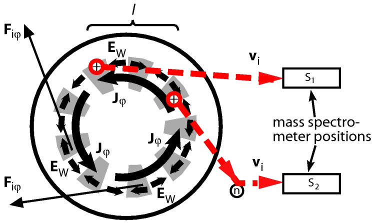

(From Lundin et al. (2008))

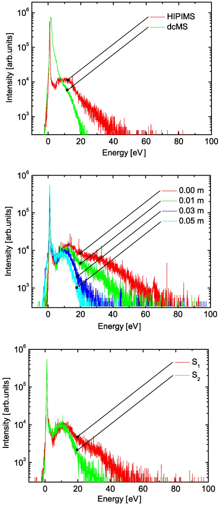

HiPIMS - Ionization fraction

- Gasless self-sputtering of copper has been demonstrated

  (Andersson and Anders, 2009)

- This self-sputtering in vacuum can deliver extraordinarily high metal-ion current
- The usable ion current increased exponentially with increasing discharge voltage

PRL **102,** 045003 (2009) PHYSICAL REVIEW LETTERS week ending 30 JANUARY 2009

Self-Sputtering Far above the Runaway Threshold: An Extraordinary Metal-Ion Generator

Joakim Andersson and André Anders

Lawrence Berkeley National Laboratory, 1 Cyclotron Road, Berkeley, California 94720, USA

(Received 12 September 2008; published 27 January 2009)

When self-sputtering is driven far above the runaway threshold voltage, energetic electrons are made available to produce "excess plasma" far from the magnetron target. Ionization balance considerations show that the secondary electrons deliver the necessary energy to the "remote" zone. Thereby, such a system can be an extraordinarily prolific generator of usable metal ions. Contrary to other known sources, the ion current to a substrate can exceed the discharge current. For gasless self-sputtering of copper, the usable ion current scales exponentially with the discharge voltage.

DOI: 10.1103/PhysRevLett.102.045003 PACS numbers: 52.80.Vp, 52.25.Jm, 52.40.Hf, 81.15.Cd

Large fluxes of ions are of interest to a number of plasma-based technologies such as self-ion assisted deposition of films and high-current and large-area ion sources. The generation of large ion fluxes is a challenging task because plasma systems tend to produce just as many ions as necessary to maintain the discharge. Hence, only a small fraction of the generated ions can be utilized for processing. Among the most prolific generators of ions are cathodic arc discharges, where the available ion current is generally quantified by normalizing it to the discharge current; the ratio is typically about 0.1 [1]. In this contribution we will demonstrate that high-power impulse magnetron sputtering (HIPIMS) can be an extremely prolific generator of metal ions that, under certain conditions, can deliver ion currents that even exceed the discharge current. We will show that this very high level is consistent with common particle and energy balance considerations.

HIPIMS was developed with the goal to at least partially ionize the sputtered atoms and thereby to provide a means for self-ion assisted deposition of thin films [2–5]. In HIPIMS, and depending on several parameters such as power density, target material, and gas pressure, the magnetron discharge plasma contains a large fraction of ionized sputtered material, and therefore HIPIMS processes are closely related to self-sputtering. Self-sputtering is an intriguing subject of research since the early reports by Hosokawa and co-workers [6,7] because, after initiating the magnetron in a gas atmosphere at high-power density, self-sputtering can sustain itself for a few target materials under certain conditions [8,9].

The *current-voltage-time* characteristics of HIPIMS discharges in background gas [10,11] show that for sufficiently long pulses (typically $>100\ \mu s$) at constant voltage, the current may go through a maximum and then settle at an equilibrium value. The current reduction after the initial peak is due to gas rarefaction. However, if the power density is high, the current evolution may look completely different in that, at a well-defined voltage threshold, the current does not reduce but jumps to a new, much higher value. This is the threshold of sustained self-sputtering [7]. At the threshold, self-sputtering amplifies itself and the self-sputtering parameter exceeds unity, $\Pi = \alpha\beta\gamma_{SS} > 1$, where α is the probability that a sputtered atom is ionized, β is the probability that the newly formed ion returns to the target, and γ_{SS} is the self-sputtering yield. All three quantities are time dependent but the system evolves towards a new steady state, with $\Pi = 1$, provided the power supply can supply the necessary current at constant voltage.

Copper is a preferred material for studying sustained self-sputtering because the sustained situation, $\Pi = 1$, can be obtained at manageable, relative low power densities (e.g., $\sim 1\ kW/cm^2$ averaged over the target area). Recently, it was shown that copper allows gasless (high vacuum) self-sputtering to occur when the magnetron discharge pulses are "kickstarted" via short vacuum-arc plasma pulses [12]. We will focus here on "gasless" sputtering because it avoids the modeling complications associated with plasmas containing both gas and metal species.

The current to a negatively biased ion collector, i.e., large probe operating in the ion saturation current, is given by the area integral over the current density $I_i = \int j_i dA$, with the Bohm current [13]

$$j_i = 0.61 n_{i0} \bar{Q} e \left(\frac{kT_{e0}}{m_i}\right)^{1/2}, \quad (1)$$

where n_{i0} is the ion density at the edge of the sheath (index "0") of the collector, $\bar{Q}$ is the mean ion charge state number, e is the elementary charge, $(kT_{e0}/m_i)^{1/2}$ is the local ion sound velocity which depends on the electron temperature, T_{e0}, and the ion mass; k is the Boltzmann constant. In the derivation of (1), the magnetic field was neglected, and it is assumed that the collector is flat, i.e., that the sheath is much thinner than the collectors curvature. There are ample descriptions of refinement in the literature [14,15] but this approximation will suffice to discuss the physics.

To determine the ion density in (1), we should consider the ion balance equation at the collector's sheath edge (omitting the index 0 for simplicity)

0031-9007/09/102(4)/045003(4) 045003-1

High Power Impulse Magnetron Sputtering (HiPIMS) - Deposition rate

HiPIMS - Deposition rate

- Several groups report on a significantly lower deposition rate for HiPIMS as compared to dcMS
  - a factor of 2 lower deposition rate for Cu and Ti thin films (Bugaev et al., 1996)
  - a factor of 4 – 7 lower deposition rate for reactive sputtering of TiO_2 from a Ti target (Davis et al., 2004)
  - a factor of 3 – 4 lower deposition rate for reactive sputtering of AlO_x from an Al target (Sproul et al., 2004)
  - the reduction in deposition rate decreases with decreased magnetic confinement (weaker magnetic field)

    (Bugaev et al., 1996)

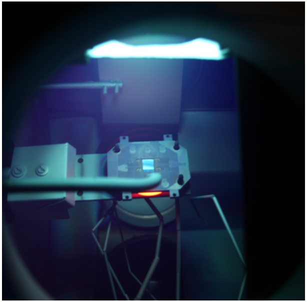

HiPIMS - Deposition rate

- One explanation is that the sputtered material is ionized close to the target and many of the metallic ions will be attracted back to the target surface by the cathode potential
  - A reduction in the deposition rate would occur mainly for metals with a low self-sputtering yield
- The deposition rate in the self sputtering mode is lower than when argon sputtering is dominating (Horwat and Anders, 2008)

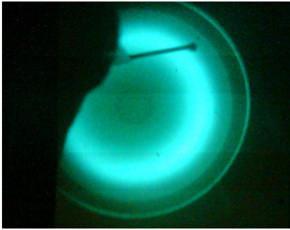

HiPIMS - Deposition rate

- It has been claimed that the magnetic confinement influences the deposition rate

  Bohlmark et al. (2006); Bugaev et al. (1996)

- A significant fraction of the ions of the sputtered material are transported sideways

  (Lundin et al., 2008)

- Also when comparing dcMS and HiPIMS discharges at the same average power the non-linear scaling of the sputter yield with the applied voltage is not taken into account

  (Emmerlich et al., 2008)

- The reduced deposition rate observed in the HiPIMS discharge is likely to be a combination of these factors

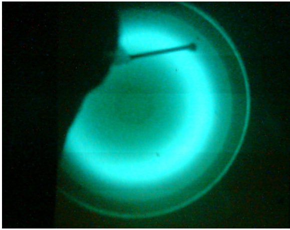

High Power Impulse Magnetron Sputtering (HiPIMS) - Applications

Application - Trench filling

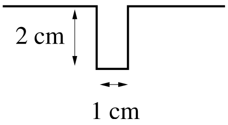

- Ta thin films grown on Si substrates placed along a wall of a 2 cm deep and 1 cm wide trench
    - conventional dc magnetron sputtering (dcMS)
    - high power impulse magnetron sputtering (HiPIMS)
- Average power is the same 440 W
- Substrate bias of - 50 V
- They were compared by scanning electron microscope (SEM), transmission electron microscope (TEM)

Application - Trench filling

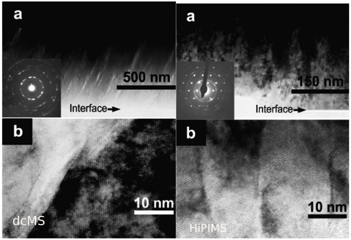

(From Alami et al. (2005))

dc magnetron HiPIMS

- dcMS grown films exhibit rough surface, pores between grains and inclined columnar structure, leaning toward the aperture
- Ta films grown by HiPIMS have smooth surface, and dense crystalline structure with grains perpendicular to the substrate

Other applications

- The advantage of high power pulsed magnetron discharge for film growth has been demonstrated by several groups
  - ultra-thin carbon films grown by HiPIMS have significantly higher densities (2.7 g/cm^3), than films grown by a conventional dcMS discharge (< 2.0 g/cm^3) Furthermore, the surface roughness is lower (DeKoven et al., 2003)
  - TiO_2 thin films grown by reactive sputtering by HiPIMS have higher index of refraction than grown by dcMS discharge - maybe due to higher density (Davis et al., 2004)
- This illustrates how the bombarding ions transfer momentum to the surface allowing the microstructure to be modified

HiPIMS - Applications

- HiPIMS has already been demonstrated on an industrial scale

  (Ehiasarian et al., 2006)

- Due to the absence of a secondary discharge in the reactor an industrial reactor can be upgraded to become IPVD device by changing the power supply

Summary

Summary

- The design parameters for Ionized Physical Vapor Deposition (IPVD) were discussed
- The high power impulse magnetron sputtering discharge (HIPIMS) has been demonstrated as an Ionized Physical Vapor Deposition (IPVD) tool
- Power supply
  - Essentially the same sputtering apparatus except for the power supply
- Electron density
  - Roughly 2 orders of magnitude higher in the substrate vicinity than for a conventional dc magnetron sputtering discharge

Summary

- Ionization fraction
  - Ionization fraction is high, mainly due to the high electron density
  - The ions on the inert gas and the ions of the sputtered vapor are separated in time
- Deposition rate
  - Deposition rate is lower than in a conventional dc magnetron sputtering discharge, maybe due to self sputtering

Acknowlegdements

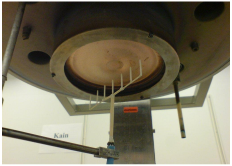

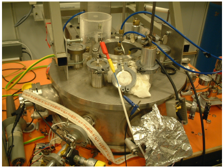

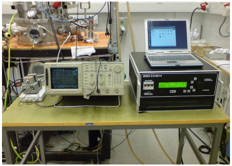

Can be downloaded at

http://www.raunvis.hi.is/~tumi/hipims.html

- This work is a result of collaboration with
  - Dr. Jones Alami (Linköping University, Sweden now Sulzer Metaplas, Germany)
  - Dr. Johan Bohlmark (Linköping University, Sweden now Sandvik A.B. Sweden)
  - Prof. Ulf Helmersson (Linköping University, Sweden)
  - Daniel Lundin (Linköping University, Sweden)
  - Petter Larsson (Linköping University, Sweden)
  - Páll Sigurjónsson (University of Iceland)
  - Kristinn B. Gylfason (University of Iceland now KTH Stockholm)
- The photographs were taken by Árni S. Ingason, Páll Sigurjónsson, Kristinn B. Gylfason and Markus Baur.
- This work was partially supported by the Icelandic Research Fund the University of Iceland Research Fund and the Swedish Research Council.

References

Alami, J., P. Eklund, J. M. Andersson, M. Lattemann, E. Wallin, J. Bohlmark, P. Persson, and U. Helmersson (2007). Phase tailoring of Ta thin films by highly ionized pulsed magnetron sputtering. *Thin Solid Films 515*(7-8), 3434–3438.

Alami, J., J. T. Gudmundsson, J. Bohlmark, J. Birch, and U. Helmersson (2005). Plasma dynamics in a highly ionized pulsed magnetron discharge. *Plasma Sources Science and Technology 14*(3), 525–531.

Alami, J., P. O. A. Petersson, D. Music, J. T. Gudmundsson, J. Bohlmark, and U. Helmersson (2005). Ion-assisted physical vapor deposition for enhanced film deposition on non-flat surfaces. *Journal of Vacuum Science and Technology A 23*(2), 278–280.

Andersson, J. and A. Anders (2009). Self-sputtering far above the runaway threshold: An extraordinary metal-ion generator. *Physical Review Letters 102*(4), 045003.

Andersson, J., A. P. Ehiasarian, and A. Anders (2008). Observation of Ti^{4+} ions in a high power impulse magnetron sputtering plasma. *Applied Physics Letters 93*(7), 071504.

Bohlmark, J., J. Alami, C. Christou, A. P. Ehiasarian, and U. Helmersson (2005). Ionization of sputtered metals in high power pulsed magnetron sputtering. *Journal of Vacuum Science and Technology A 23*(1), 18–22.

Bohlmark, J., J. T. Gudmundsson, J. Alami, M. Latteman, and U. Helmersson (2005). Spatial electron density distribution in a high-power pulsed magnetron discharge. *IEEE Transactions on Plasma Science 33*(2), 346–347.

Bohlmark, J., M. Lattemann, J. T. Gudmundsson, A. P. Ehiasarian, Y. A. Gonzalvo, N. Brenning, and U. Helmersson (2006). The ion energy distributions and ion flux composition from a high power impulse magnetron sputtering discharge. *Thin Solid Films 515*(5), 1522–1526.

Bohlmark, J., M. Östbye, M. Lattemann, H. Ljungcrantz, T. Rosell, and U. Helmersson (2006). Guiding the deposition flux in an ionized magnetron discharge. *Thin Solid Films 515*(4), 1928–1931.

Britun, N., J. G. Han, and S.-G. Oh (2008). Velocity distribution of neutral species during magnetron sputtering by Fabry-Perot interferometry. *Applied Physics Letters 92*(14), 141503.

References

Bugaev, S. P., N. N. Koval, N. S. Sochugov, and A. N. Zakharov (1996, July 21-26). Investigation of a high-current pulsed magnetron discharge initiated in the low-pressure diffuse arc plasma. In *XVIIth International Symposium on Discharges and Electrical Insulation in Vacuum, 1996*, Berkeley, CA USA, pp. 1074–1076. IEEE.

Davis, J. A., W. D. Sproul, D. J. Christie, and M. Geisler (2004). High power pulse reactive sputtering of TiO_2. In *SVC 47th Annual Technical Conferenece Proceedings*, Dallas, TX, USA, pp. 215–218. Society of Vacuum Coaters.

DeKoven, B. M., P. R. Ward, R. E. Weiss, D. J. Christie, R. A. Scholl, W. D. Sproul, F. Tomasel, and A. Anders (2003). Carbon thin film deposition using high power pulsed magnetron sputtering. In *46th Annual Technical Conferenece Proceedings*, San Francisco, CA, USA, pp. 158–165. Society of Vacuum Coaters.

Ehiasarian, A. P., R. New, W.-D. Münz, L. Hultman, U. Helmersson, and V. Kouznetzov (2002). Influence of high power densities on the composition of pulsed magnetron plasmas. *Vacuum 65*, 147–154.

Ehiasarian, A. P., C. Reinhard, P. E. Hovsepian, and J. M. Colton (2006). Industrial-scale production of corrosion-resistant CrN/NbN coatings deposited by combined high power impulse magnetron sputtering etching unbalanced magnetron sputtering deposition (HIPIMS/UBM) process. In *SVC 49th Annual Technical Conferenece Proceedings*, Washington DC, USA, pp. 349–353. Society of Vacuum Coaters.

Ehiasarian, A. P., A. Vetushka, A. Hecimovic, and S. Konstantinidis (2008). Ion composition produced by high power impulse magnetron sputtering discharges near the substrate. *Journal of Applied Physics 104*(8), 083305.

Ehiasarian, A. P., J. G. Wen, and I. Petrov (2007). Interface microstructure engineering by high power impulse magnetron sputtering for the enhancement of adhesion. *Journal of Applied Physics 101*(5), 054301.

Emmerlich, J., S. Mráz, R. Snyders, K. Jiang, and J. M. Schneider (2008). The physical reason for the apparently low deposition rate during high power pulsed magnetron sputtering. *Vacuum 82*(8), 867–870.

Gudmundsson, J. T., J. Alami, and U. Helmersson (2001). Evolution of the electron energy distribution and the plasma parameters in a pulsed magnetron discharge. *Applied Physics Letters 78*(22), 3427 – 3429.

Gudmundsson, J. T., J. Alami, and U. Helmersson (2002). Spatial and temporal behavior of the plasma parameters in a pulsed magnetron discharge. *Surface and Coatings Technology 161*(2-3), 249–256.

References

Gudmundsson, J. T., P. Sigurjonsson, P. Larsson, D. Lundin, and U. Helmersson (2009). On the electron energy in the high power impulse magnetron sputtering discharge. *Journal of Applied Physics 105*(12), 123302.

Guðmundsson, J. T., J. Bohlmark, J. Alami, K. B. Gylfason, and U. Helmersson (2005-2006). Dreifing rafeinda í tíma og rúmi í háaflpúlsaðri segulspætu. *Tímarit um raunvísindi og stærðfræði 3*(1), 75–79.

Gylfason, K. B., J. Alami, U. Helmersson, and J. T. Gudmundsson (2005). Ion-acoustic solitary waves in a pulsed magnetron sputtering discharge. *Journal of Physics D: Applied Physics 38*(18), 3417–3421.

Horwat, D. and A. Anders (2008). Spatial distribution of average charge state and deposition rate in high power impulse magnetron sputtering of copper. *Journal of Physics D: Applied Physics 41*(13), 135210.

Kouznetsov, V., K. Macák, J. M. Schneider, U. Helmersson, and I. Petrov (1999). A novel pulsed magnetron sputter technique utilizing very high target power densities. *Surface and Coatings Technology 122*(2-3), 290–293.

Kudláček, P., J. Vlekč, K. Burcalová, and J. Lukáš (2008). Highly ionized fluxes of sputtered titanium atoms in high-power pulsed magnetron discharges. *Plasma Sources Science and Technology 17*(2), 025010.

Kusano, E. (2006). Modification of film structure in pulsed and inductively-coupled-plasma assisted pulse sputtering. In *SVC 49th Annual Technical Conferenece Proceedings*, Washington, DC, USA, pp. 15–20. Society of Vacuum Coaters.

Lim, J.-W., H.-S. Park, T.-H. Park, J.-J. Lee, and J. Joo (2000). Mechanical properties of titanium nitride coatings deposited by inductively coupled plasma assisted direct current magnetron sputtering. *Journal of Vacuum Science and Technology A 18*(2), 524–528.

Lundin, D., P. Larsson, E. Wallin, M. Lattemann, N. Brenning, and U. Helmersson (2008). Cross-field ion transport during high power impulse magnetron sputtering. *Plasma Sources Science and Technology 17*(3), 035021.

Macák, K., V. Kouznetzov, J. M. Schneider, U. Helmersson, and I. Petrov (2000). Ionized sputter deposition using an extremely high plasma density pulsed magnetron discharge. *Journal of Vacuum Science and Technology A 18*(4), 1533–1537.

References

Sarakinos, K., J. Alami, and M. Wuttig (2007). Process characteristics and film properties upon growth of TiO_x films by high power pulsed magnetron sputtering. *Journal of Physics D: Applied Physics 40*(7), 2108–2114.

Sigurjonsson, P., P. Larsson, D. Lundin, U. Helmersson, and J. T. Gudmundsson (submitted 2009). Langmuir probe study of the plasma parameters in the hipims discharge. In *SVC 52nd Annual Technical Conferenece Proceedings*, Santa Clara, CA, USA. Society of Vacuum Coaters.

Sproul, W., D. J. Christie, and D. C. Carter (2004). The reactive sputter deposition of aluminum oxide coatings using high power pulsed magnetron sputtering (hppms). In *SVC 47th Annual Technical Conferenece Proceedings*, Dallas, TX, USA, pp. 96–100. Society of Vacuum Coaters.

Vašina, P., M. Meško, J. C. Imbert, M. Ganciu, C. Boisse-Laporte, L. de Poucques, M. Touzeau, D. Pagnon, and J. Bretagne (2007). Experimental study of a pre-ionized high power pulsed magnetron discharge. *Plasma Sources Science and Technology 16*(3), 501–510.

Vetushka, A. and A. P. Ehiasarian (2008). Plasma dynamic in chromium and titanium HIPIMS discharges. *Journal of Physics D: Applied Physics 41*(1), 015204.

Vlček, J., P. Kudláček, K. Burcalová, and J. Musil (2007a). High-power pulse sputtering using a magnetron with enhanced plasma confinement. *Journal of Vacuum Science and Technology A 25*(1), 42–47.

Vlček, J., P. Kudláček, K. Burcalová, and J. Musil (2007). Ion flux characteristics in high-power pulsed magnetron sputtering discharges. *Europhysics Letters 77*(4), 45002.

Wallin, E. and U. Helmersson (2008). Hysteresis-free reactive high power impulse magnetron sputtering. *Thin Solid Films 516*(18), 6398 – 6401.